ARCHIVES OF ACOUSTICS
28, 1, 43–58 (2003)

NUMERICAL ANALYSIS OF PIEZOELECTRIC PHOTOACOUSTIC SPECTRA

M. MALIŃSKI

Faculty of Electronics, Technical University of Koszalin
17 Partyzantów St, 75-411 Koszalin Poland
mmalin@tu.koszalin.pl

This paper is an introduction to the analysis of the piezoelectric photoacoustic spectra of single-layer semiconductor samples. The analysis comprises, among other things, the temperature distribution formula necessary for the computations of the piezoelectric amplitude and phase spectra. It presents also the procedures of determination of the piezoelectric spectra of semiconductor materials from the optical absorption coefficient ones and the influence of many experimental parameters on the piezoelectric spectra for semiconductors exhibiting either direct or indirect electron type transitions. The origin of the characteristic structure of the piezoelectric spectra is analyzed and discussed.

1. Introduction

The piezoelectric photoacoustic spectroscopy is one of the methods of investigation of optical parameters of solid state samples. This method is very sensitive and its main advantage over other traditional spectroscopy methods is that it directly monitors the nonradiative relaxation transitions. It is however difficult from the point of view of interpretation of the experimental results and numerical analysis of the spectra. It is, among other things, the result of complex physical processes involved in the generation of the piezoelectric signal and the complicated nonlinear relationship between the optical absorption coefficient and the amplitude and phase of the piezoelectric signal. Furthermore, the multi-layer character of real samples strongly influences the character of the spectral and frequency dependencies of the piezoelectric signal. That is the reason why the interpretation of the piezoelectric spectra was in many cases qualitative and the results have been treated to some extent by intuition.

The piezoelectric voltage signal that is generated in the piezoelectric transducer is the result of periodical heating of the sample by the modulated in intensity beam of light. The beam of light absorbed in the sample generates thermal waves that propagate in it, are reflected from its front and rear surfaces and interfere. As a result a periodical temperature field in the sample arises. This periodical temperature field causes

a periodical thermal expansion (TE) and thermoelastic bending (TEB) of the sample. The changes of the thickness and the shape of the sample are next converted into a periodical voltage signal V in the piezoelectric transducer attached to the sample.

The theory of the piezoelectric effect has been developed by JACKSON & AMER [1]. The simplified approach has been next developed by BLONSKIJ *et.al.* [2]. The single layer models presented in these papers allowed the computations of the frequency characteristics of the amplitude and phase of the piezoelectric signal and their dependencies on the optical absorption coefficient value. They did not show however the direct computation procedures leading to the characteristics of the amplitude and phase of the piezoelectric signal as a function of the energy of the exciting photons that are obtained from the measurements of the piezoelectric spectra.

The experimental piezoelectric spectra of semiconductor samples found in literature show a complex structure and a strong dependence on the technological treatment such as annealing and ion implantation [3,4,5,6,7]. The piezoelectric spectra obtained for silicon crystals exhibit also a carrier concentration dependence [8,9]. The photoacoustic piezoelectric spectroscopy has also been successfully applied to the investigation of a series of AII-BVI compounds [10,11,12].

The large number of experimental data of the piezoelectric amplitude and phase spectra in the literature brought about the necessity of a development of numerical methods of analysis of those spectra that would make the interpretation of them quantitative and would be able to clear up the physical nature of the structures observed for some of them.

The aim of this paper is to present a complex approach to the problem of numerical analysis of the piezoelectric amplitude and phase spectra comprising both the thermal and optical aspects.

2. Factors determining the analysis of the piezoelectric spectra

The analysis of the piezoelectric amplitude and phase spectra comprises a few important factors:

a) The formula for the spatial distribution of the temperature $T(x, f, l, \alpha, \beta, R)$. The amplitude, phase and instantaneous temperature distributions used in the paper are defined as follows

$$Amplitude = |T(x, f, l, \alpha, \beta, R)| \tag{1}$$

$$Phase = (180/\pi) \cdot \arg[T(x, f, l, \alpha, \beta, R)] \tag{2}$$

$$Instantaneous - Temperature = \mathrm{Re}[T(x, f, l, \alpha, \beta, R) \cdot \exp(i \cdot \omega \cdot t)] \tag{3}$$

where: x – spatial coordinate $0 < x < l$, f – frequency of modulation, l – thickness of the

sample, α – thermal diffusivity, β – optical absorption coefficient, R – thermal reflection coefficient.

b) The form of the piezoelectric equation appropriate for the experimental configuration applied $V = F(T(x,f,l,\alpha,\beta,R))$. V is the piezoelectric voltage response of the transducer that is, among other things, a function of the temperature distribution in the sample.

c) Analytical dependence of the optical absorption coefficient and the energy of exciting photons typical for the type of electron transitions in the semiconductor (direct or indirect). These dependencies are functions of several material parameters that are determined from the fitting of theoretical spectra to experimental ones.

d) The value of the thermal diffusivity taken for the computations determined from the phase spectra and the value of the thermal reflection coefficient between the sample and the backing.

3. Temperature spatial distributions

A schematic diagram of a single layer sample on a thermally thick backing material is presented in Fig. 1.

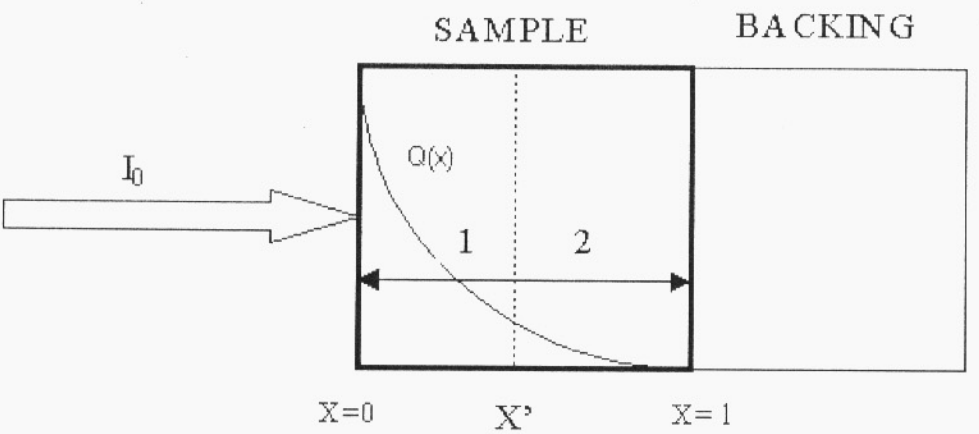

Fig. 1. Schematic diagram of a sample on the backing. I_0 is the intensity of the exciting light, 1 and 2 denote thermal waves originally travelling towards the front (1) and rear (2) side of the sample. $Q(x)$ denotes the heat distribution originally generated in the sample as a result of the optical absorption.

The backing in Fig. 1 denotes either the material of the piezoelectric transducer attached to the sample [4] or the material of the hemisphere [13,14] between the sample and the piezoelectric transducer depending on the construction of the photoacoustic (PA) piezoelectric (PZT) cell.

The temperature spatial distribution in the sample is described by the formulae [15].

$$T(x', f, l, \alpha, \beta, R) = T(x')$$

$$T(x') = \frac{\beta \cdot I_0}{2 \cdot \lambda \cdot \sigma \cdot (1 - R \cdot \exp(-2 \cdot \sigma \cdot l))} \cdot [M(x') + N(x')]$$

$$M(x') = \frac{[\exp(\sigma \cdot x') + \exp(-\sigma \cdot x')] \cdot [\exp((-\sigma - \beta) \cdot x') - \exp((-\sigma - \beta) \cdot l)]}{\beta + \sigma} \tag{4}$$

$$+ \frac{R \cdot \exp(-2 \cdot \sigma \cdot l) \cdot [\exp(\sigma \cdot x') + \exp(-\sigma \cdot x')] \cdot [\exp((\sigma - \beta) \cdot x') - \exp((\sigma - \beta) \cdot l)]}{\beta - \sigma}$$

$$N(x') = \frac{[\exp(-\sigma \cdot x') + R \cdot \exp(-2 \cdot \sigma \cdot l + \sigma \cdot x')] \cdot [1 - \exp((-\sigma - \beta) \cdot x')]}{\beta + \sigma}$$

$$+ \frac{[\exp(-\sigma \cdot x') + R \cdot \exp(-2 \cdot \sigma \cdot l + \sigma \cdot x')] \cdot [1 - \exp((\sigma - \beta) \cdot x')]}{\beta - \sigma}$$

where: $\sigma = (1 + i) \cdot \sqrt{\pi \cdot f / \alpha}$ and λ is the thermal conductivity of the sample.

Examples of the instantaneous temperature distributions in the semiconductor sample on the thermally insulating ($R = 1$) and thermally conducting ($R = -1$) backing are presented in Figs. 2a and 2b, respectively.

a)

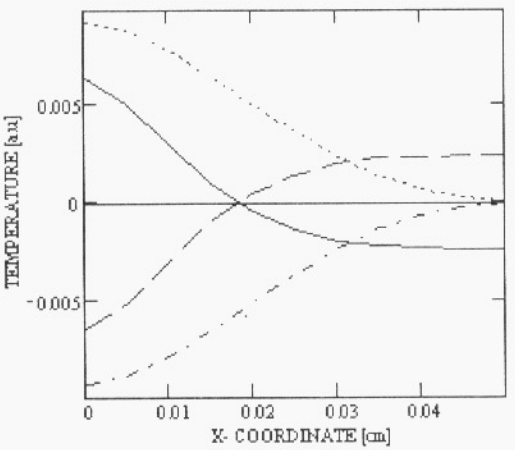

[Fig.2 (a)]

b)

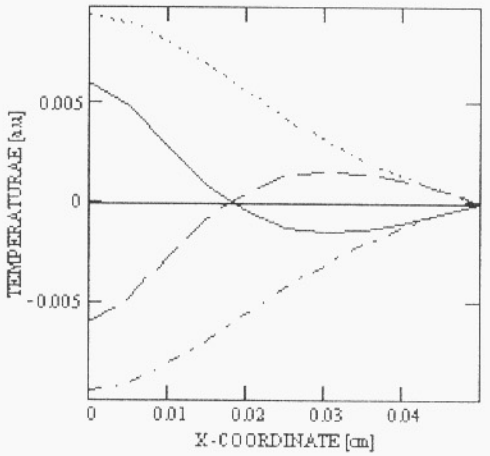

Fig. 2. Spatial distributions of the instantaneous temperature in the sample, (a) Parameters: $R = 1$, $l = 500$ μm, $f = 77$ Hz, $\alpha = 0.1$ cm^2/s, $\beta = 200$ cm^{-1}. Description of lines: solid line $t = 0$, dotted $t = T/4$, dash $t = T/2$, dash-dot $t = 3T/4$. T denotes the period of excitation, t is the time delay against the excitation, (b) Parameters: $R = -1$, $l = 500$ μm, $f = 77$ Hz, $\alpha = 0.1$ cm^2/s, $\beta = 200$ cm^{-1}. Description of lines: solid line $t = 0$, dotted $t = T/4$, dash $t = T/2$, dash-dot $t = 3T/4$. T denotes the period of excitation, t is the time delay against the excitation.

The spatial distributions of the amplitude and phase of the temperature for the same sample as in Figs. 2a and 2b are presented in Figs. 3a, 3b, 3c and 3d.

The value of the piezoelectric signal depends first of all on the temperature distribution in the sample. Figures 2 a, b and 3 a, b, c, d clearly show the considerable influence of the thermal properties of the backing (thermally insulating ($R = 1$) or thermally conducting ($R = -1$)), on the temperature distribution in the sample. From

a)

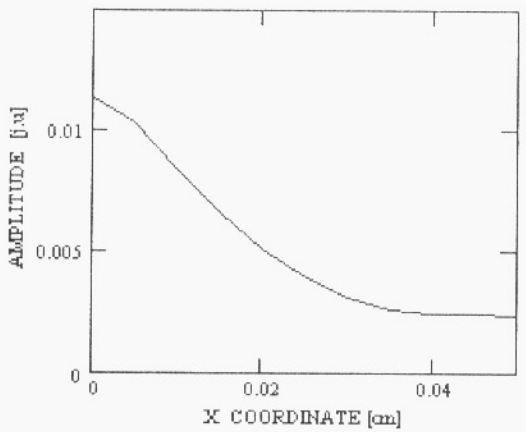

[Fig. 3 (a)]

b)

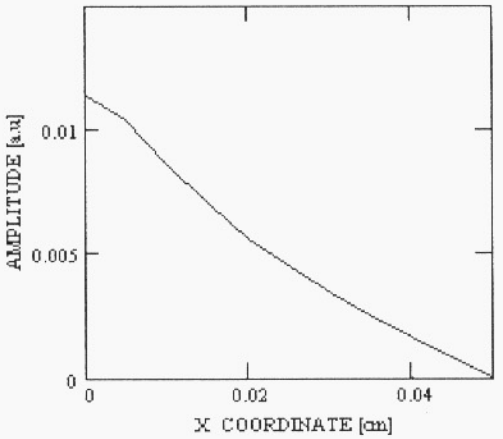
AMPLITUDE [a.u]
0.01
0.005
0
0
0.02
0.04
X COORDINATE [cm]

c)

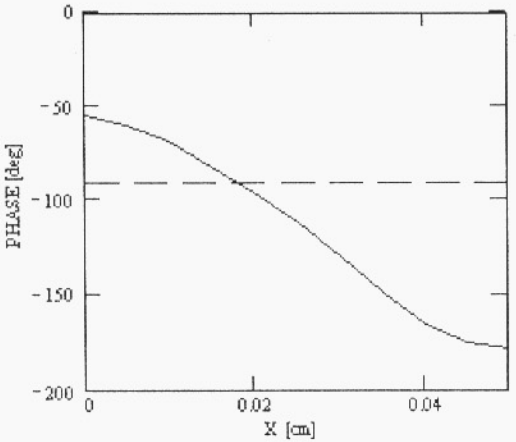
0
-50
-100
-150
-200
PHASE [deg]
0
0.02
0.04
X [cm]

[Figs. 3 (b), (c)]

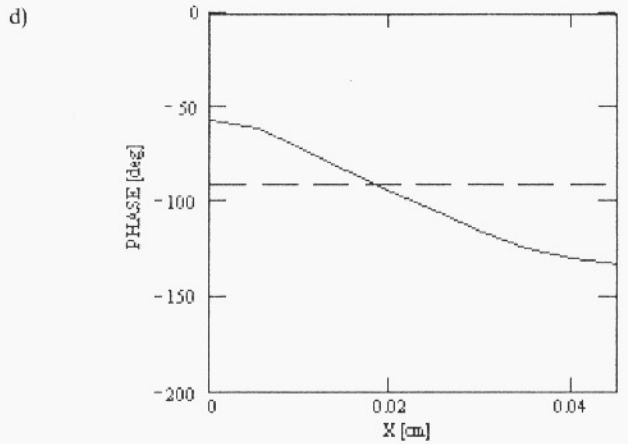

Fig. 3. Temperature amplitude distribution in the sample, (a) Parameters: $R = 1$, $l = 500$ μm, $f = 77$ Hz, $\alpha = 0.1$ cm^2/s, $\beta = 200$ cm^{-1}, (b) Parameters: $R = -1$, $l = 500$ μm, $f = 77$ Hz, $\alpha = 0.1$ cm^2/s, $\beta = 200$ cm^{-1}, (c) Parameters: $R = 1$, $l = 500$ μm, $f = 77$ Hz, $\alpha = 0.1$ cm^2/s, $\beta = 200$ cm^{-1}, (d) Parameters: $R = -1$, $l = 500$ μm, $f = 77$ Hz, $\alpha = 0.1$ cm^2/s, $\beta = 200$ cm^{-1}

the results of the analysis presented above, one can draw the conclusion that the value of the R parameter should be clearly indicated for the purpose of the numerical analysis of the piezoelectric spectra.

4. Piezoelectric equation

For the computations of the piezoelectric spectra, the JACKSON & AMER modified equation for the piezoelectric voltage response in the front experimental configuration was applied. It is given by the formula (5).

$$V \approx \varepsilon \cdot S \cdot k \cdot \gamma \cdot \left(\frac{1}{l} \cdot \int_0^1 T(x) \cdot dx - \frac{1}{2 \cdot r^2} \cdot \int_0^1 \left(\frac{l}{2} - x\right) \cdot T(x) \cdot dx\right) \cdot (-1) \tag{5}$$

where $r = l/2 \cdot \sqrt{3}$, ε – force-voltage conversion factor of the piezoelectric transducer, S – surface of the sample, k – longitudinal modulus of elasticity (Young's modulus), γ – coefficient of thermal expansion, l – the thickness of the sample, $T(x)$ – temperature distribution in the sample.

The first part of equation (5) describes the contribution of the thermal linear expansion of the sample to the piezoelectric voltage. The second one describes the thermoelastic bending contribution of the sample to the piezoelectric voltage.

Thus equation (5) can be rewritten in a short form as the difference of the TE and TEB contributions as follows:

$$V \approx TE - TEB \tag{6}$$

The $T(x)$ spatial temperature distribution in the formula (5), used for the computations in this paper, is described by the formulae (4). The JACKSON & AMER equation (5) enables the computations of the complex piezoelectric voltage response of

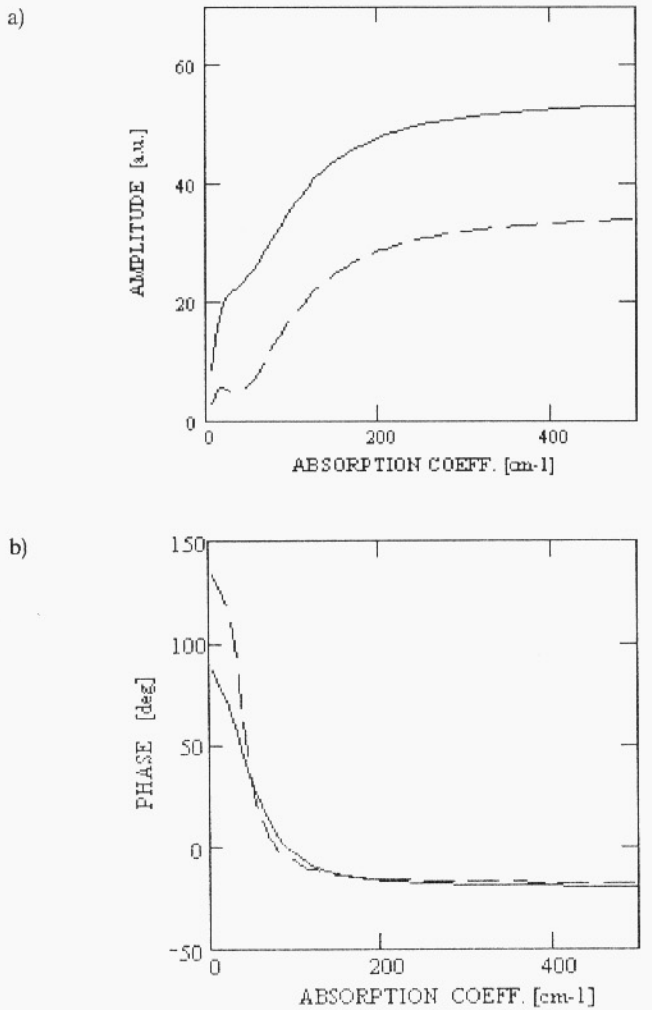

Fig. 4. Amplitude of the piezoelectric signal versus the optical absorption coefficient, (a) Parameters: $l = 500$ μm, $\alpha = 0.1$ cm^2/s, $f = 77$ Hz. Solid line $R = 1$, dash line $R = -1$, (b) Solid line $R = 1$, dash line $R = -1$, $l = 500$ μm, $\alpha = 0.1$ cm^2/s, $f = 77$ Hz.

the piezoelectric transducer as a function of the value of the optical absorption coefficient for a given frequency of modulation or as a function of the frequency of modulation for a given value of the optical absorption coefficient.

The literature piezoelectric spectroscopy data show [3–12] that the piezoelectric spectra depend on the frequency of modulation. Examples of the amplitude and phase characteristics versus the optical absorption coefficient and frequencies $f = 77$ Hz and $f = 400$ Hz are presented in Fig. 4a, b and Fig. 5a, b respectively.

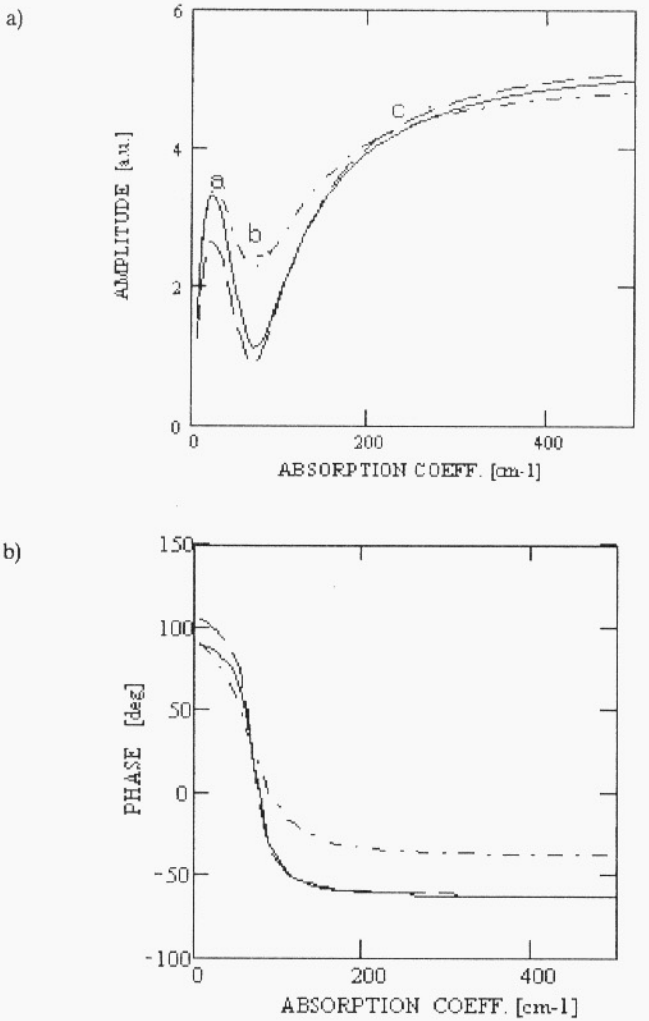

Fig. 5. Amplitude of the piezoelectric signal versus the optical absorption coefficient, (a) Solid line – $R = 1$, $\alpha = 0.1$ cm^2/s, dash line – $R = -1$, $\alpha = 0.1$ cm^2/s, dashdot line $R = 1$, $\alpha = 0.24$ cm^2/s. Other parameters: $l = 500$ μm, $f = 400$ Hz, (b) Solid line – $R = 1$, $\alpha = 0.1$ cm^2/s, dash line – $R = -1$, $\alpha = 0.1$ cm^2/s, dash-dot line $R = 1$, $\alpha = 0.24$ cm^2/s. Other parameters: $l = 500$ μm, $f = 400$ Hz.

The amplitude spectra presented in Figs. 4a and 5a exhibit some characteristic features worthwhile noting and discussing since they appear always in the piezoelectric spectra. They are denoted as a, b and c in Fig. 5a. The (a) peak always appears for the low optical absorption coefficient where the TE contribution to the piezoelectric signal is always larger than the TEB one. The TE contribution dominates as the sample exhibits a uniform temperature distribution with no temperature gradient. Point (b), called 'dip' in the literature, appears for the optical absorption value when the TE and TEB contributions are equal and TE-TEB reaches its minimum value. Point (c) denotes the saturation region where the TEB contribution dominates and the samples exhibit a strong temperature gradient.

5. The dependence of the optical absorption coefficient on the energy of photons

In the photoacoustic spectroscopy (PAS) experiments, the amplitude and phase characteristics of the piezoelectric signal as functions of the energy of exciting photons or the wavelength of the exciting light are measured. For the purpose of the numerical analysis of the spectra a functional dependence of the optical absorption coefficient versus the energy of absorbed photons is required. The formulae necessary for the computations in the case of direct and indirect electron type transitions are presented below (7) and (8).

5.1. Direct electron type transitions

$$E_{exc} < E_g \qquad\qquad E_{exc} > E_g$$

$$\beta(h\nu) = \beta_0 \cdot \exp\left(\frac{(E_{exc} - E_g)\cdot\gamma)}{k \cdot T}\right) \qquad \beta(h\nu) = A_0 \cdot \sqrt{E_{exc} - E_g} + \beta_0 \qquad (7)$$

where: E_g – energy gap at the temperature T, γ – broadening parameter, k – Boltzmann constant, E_{exc} – energy of exciting photons, β_0, A_0 – absorption factors.

For $E_{exc} < E_g$ (the low absorption region) the samples exhibit an exponential character of $\beta(h \cdot \nu)$ called the Urbach edge, while for $E_{exc} > E_g$ (the high absorption region) they exhibit an optical absorption dependence characteristic for the vertical allowed transitions in a quantum mechanical sense [16, 17].

An exemplary characteristic of the optical absorption coefficient versus photon energy used for the computations of the piezoelectric spectra and typical of the direct electron type transitions is presented in Fig. 6.

The influence of the Urbach edge region on the photoacoustic spectra has already been analyzed in the microphone detection measuring method [18–21]. The influence

of this absorption region on the piezoelectric photoacoustic spectra is considerably different and is analyzed below.

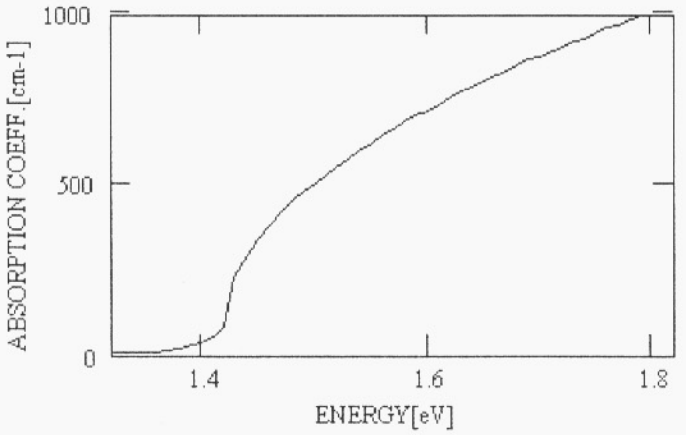

Fig. 6. Optical absorption coefficient spectrum used for the computations, typical of the direct type transitions. Parameters of the spectrum: $Eg = 1.42$ eV, $\beta o = 80$ cm^{-1}, $\gamma = 1$, $A_0 = 1500$ cm^{-1}/eV$^{-1/2}$, $T = 300$K.

5.2. Indirect electron type transitions

For the case of indirect type transitions, with emission of phonons, the optical absorption coefficient spectrum can be described in the form (5.2) where E_{ph} is the energy of the phonon involved in the electron transition and A_0 is the absorption factor:

$$\beta(h \cdot v) = \frac{A_0 \cdot [E_{exc} - E_g - E_{ph}]^2}{1 - \exp(-E_{ph}/k \cdot T)} \tag{8}$$

This form of dependence, applied for the computations of the piezoelectric spectra, is a simplified form of the optical absorption spectrum but verified by the experimental results taken from the literature [22–24].

The example characteristic of the optical absorption coefficient versus the photon energy typical of the indirect electron type transitions and applied for the computations of the piezoelectric spectra is presented in Fig. 7.

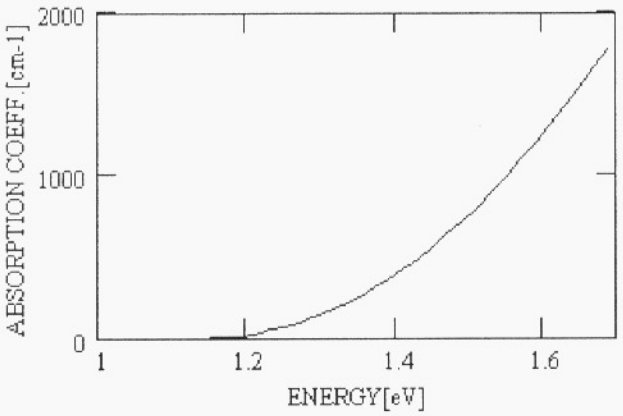

Fig. 7. Optical absorption coefficient spectrum, taken for computations, typical of the indirect type transitions. Parameters of the spectrum: $Eg = 1.09$ eV, $A_0 = 5125$ cm^{-1}/eV^2, $E_{ph} = 50.8$ meV, $T = 300$K.

6. Computations and discussion of the piezoelectric spectra

The results of computations of the amplitude and phase piezoelectric spectra for the sample exhibiting the direct type transitions and of the optical absorption spectrum presented in Fig. 6 for different frequencies of modulations are presented in Figs. 8a and 8b.

The results of computations of the amplitude and phase of the piezoelectric spectra for the sample exhibiting indirect type transitions and the optical absorption spectrum presented in Fig. 7 for different frequencies of modulations are presented in Figs. 9a and 9b.

All the amplitude spectra exhibit a similar character and the changes are only quantitative. The origin of the peaks and dips observed in the spectra can be well explained as a result of different TE and TEB contributions. These contributions, computed for the sample whose amplitude spectrum is presented in Fig. 8a, are presented in Fig. 10 as a function of the energy of the exciting photons. The symbols *'a'*, *'b'*, *'c'*, have the same meanings as in Fig. 5a. For the energies below the energy gap of the semiconductor (low absorption region), the TE (thermal expansion) contribution dominates. In point *'a'*, where the difference of TE-TEB is the biggest, a local maximum below the energy gap is observed in the piezoelectric spectrum. Point *'b'* is the place where the contributions TE and TEB are equal and the spectrum exhibits local minimum called 'dip'. Point *'c'* for the higher absorption region indicates the region

where the TEB (thermoelastic bending) effect dominates and the piezoelectric spectrum reaches the saturation range.

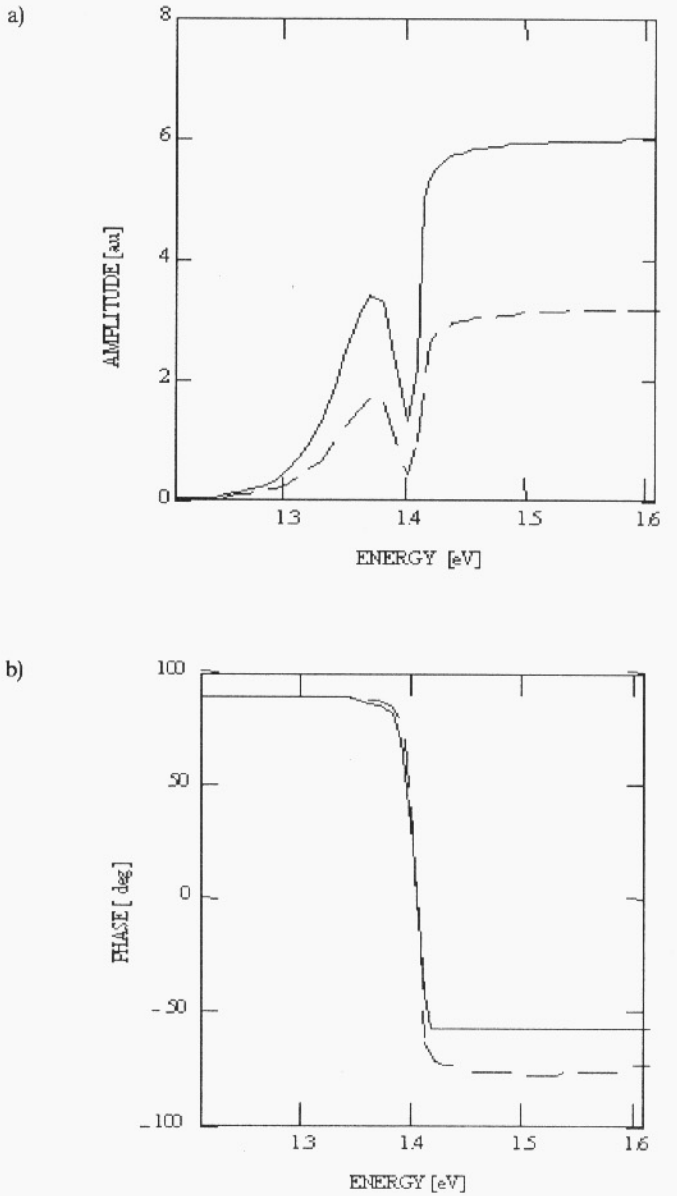

Fig. 8. a) Amplitude of the piezoelectric signal versus the photon energy for a sample exhibiting direct type transitions and $l = 500$ μm, $\alpha = 0.1$ cm^2/s, $f = 400$ Hz (solid line) and $f = 800$ Hz (dash line), $R = 1$, b) Phase of the piezoelectric signal versus the photon energy for the sample $l = 500$ μm, $\alpha = 0.1$ cm^2/s, $f = 400$ Hz (solid line) and $f = 800$ Hz (dash line), $R = 1$.

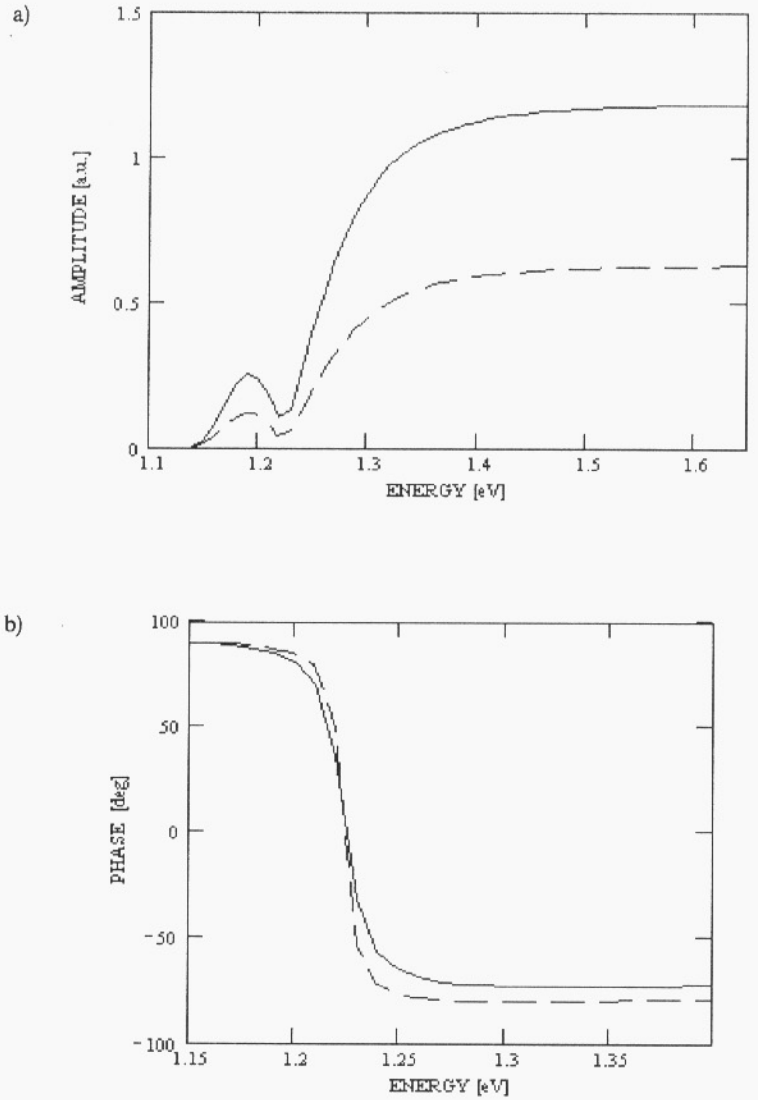

Fig. 9. a) Amplitude of the piezoelectric signal versus the photon energy for the sample exhibiting indirect type transitions; $l = 500\ \mu m$, $\alpha = 0.1\ cm^2/s$, $f = 400$ Hz (solid line) and $f = 800$ Hz (dash line), $R = 1$, b) Phase of the piezoelectric signal versus the photon energy for a sample exhibiting indirect electron type transitions; $l = 500\ \mu m$, $\alpha = 0.1\ cm^2/s$, $f = 400$ Hz (solid line) and $f = 800$ Hz (dash line), $R = 1$.

Those characteristic points and structures were observed experimentally for the following materials after different technological treatment: GaAs, InSe, *p* and *n* type Si [3–9] and a series of AII-BVI mixed crystals [10–12]. The application of the procedures described above enables the computations of the optical absorption

coefficient spectra of these materials when the optical parameters are treated as fitting parameters and the thermal parameters of the samples are known.

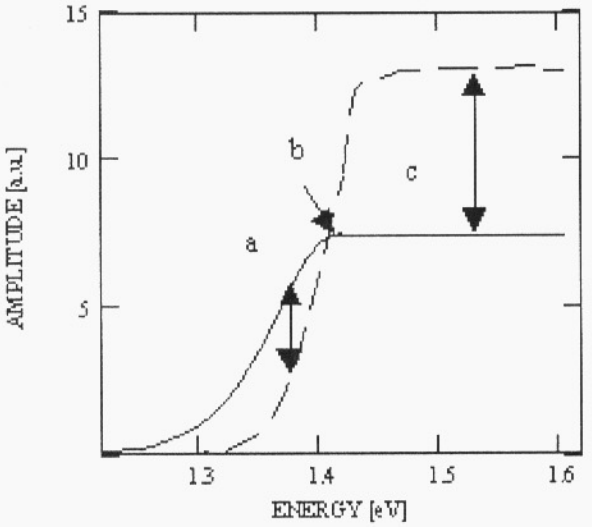

Fig. 10. TE (solid line) and TEB (dash line) contributions as a function of the photon energy for a semiconductor exhibiting direct electron type transition, the optical absorption coefficient spectrum presented in Fig. 6 and the piezoelectric amplitude spectrum presented in Fig. 8a.

7. Conclusions

The model presented in this paper enables the computations of both the amplitude and phase piezoelectric spectra for all semiconductor materials exhibiting either direct or indirect electron type transitions. The results of the analysis presented convey an nisight into the nature of the characteristic structure observed for all the piezoelectric amplitude spectra. The computations performed indicated that the structure observed is the result of the respective changes of the TE and TEB contributions with the optical absorption coefficient. This paper also shows the application of the proposed temperature distribution formula in the field of the piezoelectric spectroscopy.

References

[1] W. JACKSON, N.M. AMER, *Piezoelectric photoacoustic detection: theory and experiment*, J. Appl. Phys., 51(6), 3343–3353, (1980).

[2] J.V. BLONSKIJ, V.A. TKHORYK, M.L. SHENDELEVA, *Thermal diffusivity of solids determination by piezoelectric technique*, J. Appl. Phys., 79(7), 3512–3516, (1996).

[3] T. IKARI, K. MIYAZAKI, A. FUKUYAMA, H. YOKOYAMA, K. MAEDA, K. FUTUGAMI, Piezoelectric detection of the photoacoustic signals of *n*-type GaAs single crystals, J. Appl. Phys., 71(5), 2408–2413, (1991).

[4] S. SHIGETOMI, T. IKARI, Y. YOGA, S. SHIGETOMI, *Annealing behavior of photoacoustic spectra of undoped InSe*, Phys. Stat. Sol.(a), 90, K61–K64, (1985).

[5] T. IKARI, H. YOKOYAMA, S. SHIGETOMI, K. FUTUGAMI, *Near band edge photoacoustic spectra of p-Si single crystals*, Jpn. J. Appl. Phys., 29(5), 887–890, (1990).

[6] T. IKARI, K. MAEDA, K. FUTUGAMI, *Photoacoustic signals from ion implanted and epitaxially grown layers on silicon substrate*, Jpn. J. Appl. Phys., 33,2,(3A), L351–L353, (1994).

[7] K. HIHASHI, T. IKARI, H. YOKOYAMA, K. FUTAGAMI, *Effect on thermal donor formation on the photoacoustic spectra of p-Si single crystals*, Jpn. J. Appl. Phys., 32,1,(5B), 2570–2572, (1993).

[8] H. KUWAHATA, N. MUTO, F. UEHARA, *Carrier concentration dependence of photoacoustic spectra of silicon by a piezoelectric transducer method*, Jpn. J. Appl. Phys., 39, 3169–3171, (2000).

[9] H. KUWAHATA, N. MUTO, F. UEHARA, *Carrier concentration dependence of photoacoustic spectra of n-type silicon by microphone and piezoelectric transducer method*, Anal. Sciences, 17, 31–34, (2001).

[10] F. FIRSZT, S. ŁĘGOWSKI, H. MĘCZYŃSKA, J. SZATKOWSKI, J. ZAKRZEWSKI, *Photoacoustic study of* $Zn_{1-x}Be_xSe$ *mixed crystals*, AIP Conf. Proc. 463- 10th ICPPP, 350–352, (1999).

[11] F. FIRSZT, S. ŁĘGOWSKI, H. MĘCZYŃSKA, J. SZATKOWSKI, J. ZAKRZEWSKI, *Photoacoustic study of* $Zn_{1-x}Be_xTe$ *mixed crystals*, Analytical Sciences 17, 129–132, (2001).

[12] W. PASZKOWICZ, F. FIRSZT, S. ŁĘGOWSKI, H. MĘCZYŃSKA, J. ZAKRZEWSKI, M. MARCZAK, *Structural, optical and thermal properties of bulk* $Zn_{1-x}Be_xTe$ *crystals*, Phys. stat. sol. (b) 229 No. 1, 57–62, (2002).

[13] H.D. BREUER, Proc. 1st Int. Conf. On Photoacoustic Effect in Germany, Vieg & Son, 115–117, (1981).

[14] J. ZAKRZEWSKI, PhD Thesis UMK Toruń (2001).

[15] M. MALIŃSKI, *Temperature distribution formulae-applications in photoacoustics*, Archives of Acoustics 27, 3, 217–228, (2002).

[16] J.I. PANKOVE, *Optical processes in semiconductors*, WNT, Warszawa (1974).

[17] N.F. MOTT, E.A. DAVIS, *Electronic processes in non-crystalline materials*, Clarendon, Oxford (1979).

[18] A.K. GHOSH, K.K. SOM, S. CHATTERJEE, B.K. CHAUDHURI, *Photoacoustic spectroscopic study of energy gap, optical absorption, and thermal diffusivity of polycrystalline* $ZnSe_xTe_{1-x}$ *alloys*, Phys. Rev. B, 51(8), 4842–4848, (1995).

[19] M. MALIŃSKI, L. BYCHTO, S. ŁĘGOWSKI, J. SZATKOWSKI, J. ZAKRZEWSKI, *Photoacoustic studies of* $Zn_{1-x}Be_xSe$ *mixed crystals: two-layer approach*, Micro. Journ., 32, 903–910, (2001).

[20] M. MALIŃSKI, L. BYCHTO, S. ŁĘGOWSKI, J. SZATKOWSKI, J. ZAKRZEWSKI, *Photoacoustic spectroscopy studies of* $Zn_{1-x}Be_xSe$ *mixed crystals*, Proc. 6th Therminic Workshop Budapest, 93–96, (2000).

[21] M. MALIŃSKI, L. BYCHTO, F. FIRSZT, J. SZATKOWSKI, J. ZAKRZEWSKI, *Determination of the optical absorption coefficient of* $Zn_{1-xy}Be_xMg_ySe$ *mixed crystals from the PAS experiments-improved approach*, Anal. Scien., 17, 133–136, (2001).

[22] J.E. POKROWSKI [Ed.], *Radiant recombination in semiconductors*, PWN, 53–63, (1975).

[23] J.M. SERRA, R. GAMBOA, A.M. VALLERA, *Optical absorption coefficient of polycrystalline silicon with very high oxygen content*, Mat. Science. & Eng., B-Solid State Mat. For Adv. Techn, 36(1–3), 73–76, (1996).

[24] M. MALIŃSKI, L. BYCHTO, A. PATRIN, *Near band edge photoacoustic spectra of n-Si and p-Si single crystals*, Proc. 23rd IMAPS Poland Conf., 81–85, (1999).